Journal of Alloys and Compounds 503 (2010) L14–L17

Contents lists available at ScienceDirect

Journal of Alloys and Compounds

journal homepage: www.elsevier.com/locate/jallcom

Letter

Photoluminescence and concentration quenching of $NaCa_4(BO_3)_3$:Eu^{3+} phosphor

Xinmin Zhang[a], Hyo Jin Seo[b,*]

[a] School of Materials Science and Engineering, Central South University of Forestry and Technology, Changsha 410004, China
[b] Department of Physics, Pukyong National University, 599-1,Daeyeon 3-Dong, Nam-Gu, Busan 608-737, Republic of Korea

ARTICLE INFO

Article history:
Received 25 February 2010
Received in revised form 27 April 2010
Accepted 29 April 2010
Available online 6 May 2010

Keywords:
Phosphors
Solid-state reactions
Optical properties
Luminescence

ABSTRACT

Novel Eu^{3+}-doped $NaCa_4(BO_3)_3$ phosphors were synthesized by solid-state reactions. The emission spectra exhibit well-known transitions from the $^5D_0$ level to the lower ^7F manifold. The excitation spectrum monitored with 613 nm consists of broad excitation band peaking at 265 nm and some narrow lines originated from the typical Eu^{3+} intra-$4f^6$ transitions. The optimum Eu^{3+} doped concentration, the critical distance of the concentration quenching, the fluorescence decay curves, and the mechanism of concentration quenching are investigated.

1. Introduction

The photoluminescence properties of rare earth ions in borates have been studied extensively due to their application in the fields of fluorescent lamps, display devices, and detector systems [1–4]. Recently, the borate phosphors have attracted great attention due to their potential application in white lighting emitting diodes (white LEDs) and related fields [5–10].

Recently, a series of new borates with the composition of $MM_4'(BO_3)_3$ (M = Li, Na, K; M′ = Ca, Sr, Ba) was discovered [11]. The crystal structure and photoluminescence properties of the polycrystal doped with rare earths ions were investigated. Jiang et al. studied the synthesis, photoluminescence, thermoluminescence and dosimetry properties of novel phosphors ($NaSr_4(BO_3)_3$:Ce^{3+}, $KSr_4(BO_3)_3$:Ce^{3+}) under β-ray irradiation [3,12]. In borates, Eu^{3+} and Tb^{3+} ions can show high luminescence efficiency under ultraviolet excitation [2,13]. The energy levels of Eu^{3+} have been fully investigated. Because the visible emission of Eu^{3+} ion in 4f shell is insensitive to the influence of the surroundings due to the shielding effect of 5 s, 5p electron, the luminescence properties of Eu^{3+} ions are strongly related to their chemical and structural environment inside the host matrix [14–16].

The present paper deals with the emission and excitation spectra of Eu^{3+} in the $NaCa_4(BO_3)_3$ crystal together with an analysis of the mechanism of concentration quenching of Eu^{3+} emission for the first time.

2. Experimental

Samples of $NaCa_{4-2x}(BO_3)_3$:xEu^{3+},xNa^+ were prepared according to the standard solid-state technique. High-purity starting materials Na_2CO_3 (Aldrich, 99.9%), $CaCO_3$ (Aldrich, 99.9%), H_3BO_3 (Aldrich, 99.9%, 10 mol% excess to compensate the evaporation in the heating processes), and Eu_2O_3 (Aldrich, 99.99%) were used. The well-mixed materials were annealed at 880 °C for 12 h in air with an intermediate grinding. Na^+ was added as a charge compensator. The structural characteristics of $NaCa_{4-2x}(BO_3)_3$:xEu^{3+},xNa^+ samples were checked by X-ray diffraction (XRD) patterns using a Philips XPert/MPD diffraction system with Cu Kα (λ = 0.15405 nm) radiation. The photoluminescence emission and excitation spectra were performed at room temperature using spectrometer (Photo Technology International) with a 150 W Xe lamp as an excitation source. The luminescence decays were measured by monitoring the given emission from the samples under 266 nm pulsed laser excitation. Decay profiles were recorded with a LeCloy 9301 digital storage oscilloscope in which the signal was fed from PMT.

3. Results and discussion

Fig. 1 shows the powder X-ray diffraction pattern of $NaCa_{3.999}(BO_3)_3$:0.0005Eu^{3+},0.0005Na^+ sample. The $NaCa_4(BO_3)_3$ compound crystallizes in the noncentrosymmetric space group *Ama*2 with lattice parameters: $a = 1.06800(1)$ nm, $b = 1.12857(1)$ nm and $c = 0.64852(6)$ nm. The Ca atoms occupy three different sites [11]. All of the diffraction peaks are in good agreement with the result in Ref. [11].

Eu^{3+} doped $NaCa_4(BO_3)_3$ phosphors show red emission at room temperature under ultraviolet excitation. Fig. 2 shows the photoluminescence (PL) emission and excitation spectra of

* Corresponding author. Tel.: +82 51 629 5568; fax: +82 51 629 5549.
E-mail address: hjseo@pknu.ac.kr (H.J. Seo).

0925-8388/$ – see front matter © 2010 Elsevier B.V. All rights reserved.
doi:10.1016/j.jallcom.2010.04.242

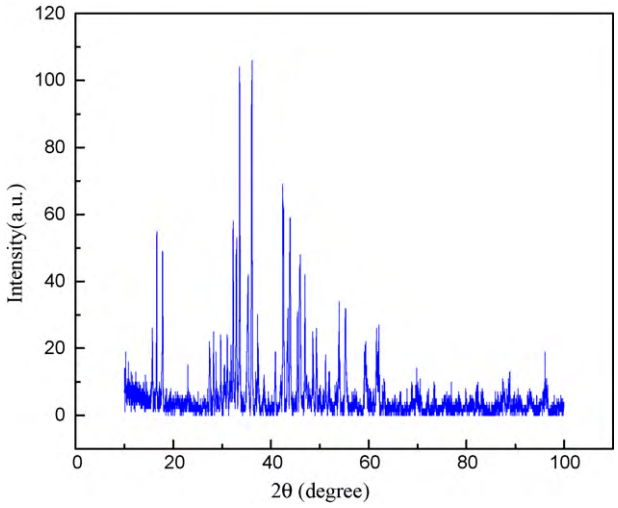

Fig. 1. XRD pattern of $NaCa_{3.999}(BO_3)_3$:0.0005Eu^{3+},0.0005Na^+.

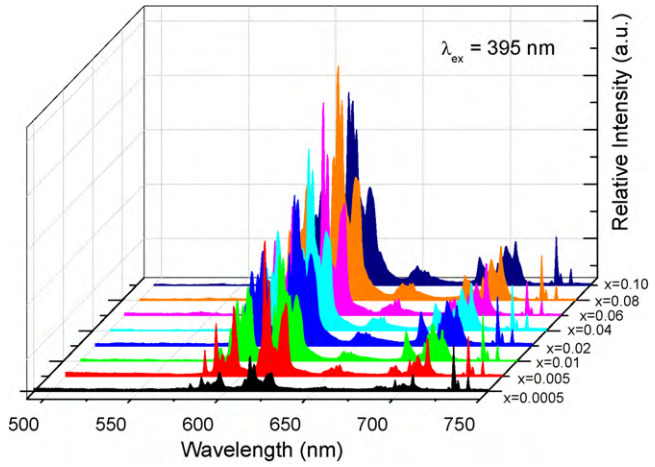

Fig. 3. Eu^{3+} concentration dependence of emission spectra of $NaCa_{4-2x}(BO_3)_3$:xEu^{3+},xNa^+.

$NaCa_{4-2x}(BO_3)_3$:xEu^{3+},xNa^+. Under 265 and 395 nm excitation, the Eu^{3+} emission consists of the well-known transitions from the $^5D_0$ level to the lower ^7F manifold. The emission peaks observed at 580, 590, 612, 650, and 698 nm are assigned to the transition $^5D_0 \rightarrow {}^7F_0$, $^5D_0 \rightarrow {}^7F_1$, $^5D_0 \rightarrow {}^7F_2$, $^5D_0 \rightarrow {}^7F_3$, and $^5D_0 \rightarrow {}^7F_4$, respectively. Moreover, there are two extra emission bands under 254 nm UV excitation (they are marked with asterisk in the Fig. 2). These bands may be assigned to self-trapped exciton (STE) in the host lattice [11,17]. In fact, the undoped $NaCa_4(BO_3)_3$ emits blue light when excited with 254 nm UV lamp, and the emission spectrum is shown in the inset of Fig. 2.

The excitation spectrum monitored with 613 nm consists of broad excitation band peaking at 265 nm and some narrow lines. The excitation band should be assigned to the charge transfer transition of Eu^{3+}–O^{2-} [18]. The absorption of BO_3 groups may be situated at higher energy level [18,19]. The narrow peaks are attributed to the typical Eu^{3+} intra-$4f^6$ transitions, including the peaks with maxima at 320 nm ($^7F_0$–^5H_J), 396 nm ($^7F_0$–$^5L_6$), and 465 nm ($^7F_0$–$^5D_2$).

The emission intensity dependence on the Eu^{3+} concentration is shown in Fig. 3. The emission intensity of phosphors increases with increasing Eu^{3+} concentration, and the maximum intensity approaches at $x = 0.08$, then concentration quenching takes place. In this case, the energy transfer occurs from one activator to another until an energy sink in the lattice is reached. So it is possible to obtain the critical distance (R_0) from the concentration quenching data. R_0 is, in fact, the critical separation between donor (activator ion) and acceptor (quenching ion), at which the nonradiative rate equals that of the internal single ion relaxation. Blasse assumed that for the critical concentration the average shortest distance between nearest activator ions is equal to the critical distance R_0. The R_0 value can be practically calculated using the following equation [20]

$$R_0 = 2 \times \left(\frac{3V}{4\pi x_C N}\right)^{1/3} \quad (1)$$

where x_C is the critical concentration, N the number of Ca^{2+} ions in the $NaCa_4(BO_3)_3$ unit cell, and V the volume of the unit cell. Using the above equation, the critical distance is determined to be about 16.7 Å for the critical concentration.

As we mentioned before the emission intensity decreases as Eu^{3+} concentration is greater than 0.08. In order to investigate the concentration quenching behavior of the Eu^{3+} emission, the fluorescence decay curves with pulsed excitation at 266 nm are examined in terms of Eu^{3+} concentration, and they are shown in Fig. 4. It can be seen that the concentration quenching is also made evident by the change from exponential to non-exponential decays

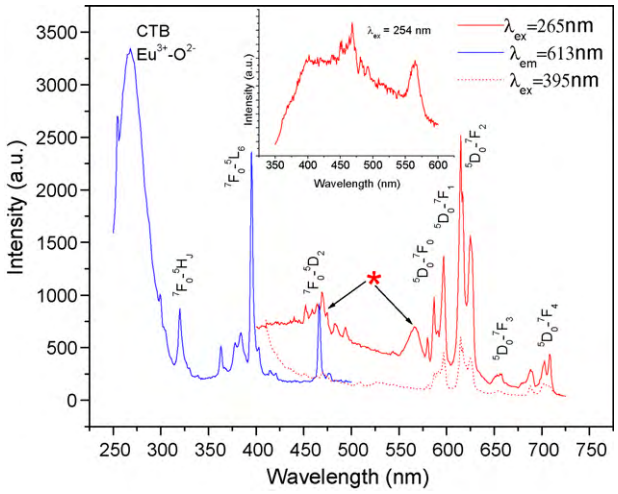

Fig. 2. PL emission and excitation spectra of $NaCa_4(BO_3)_3$:Eu^{3+},Na^+(the inset shows the emission spectrum of $NaCa_4(BO_3)_3$ excited with 254 nm UV).

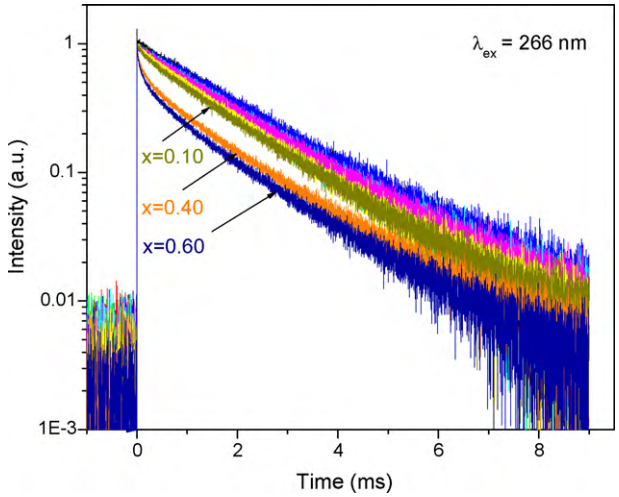

Fig. 4. Decay curves of $^5D_0$–$^7F_2$ transition under 266 nm pulsed laser excitation for $NaCa_{4-2x}(BO_3)_3$:xEu^{3+},xNa^+.

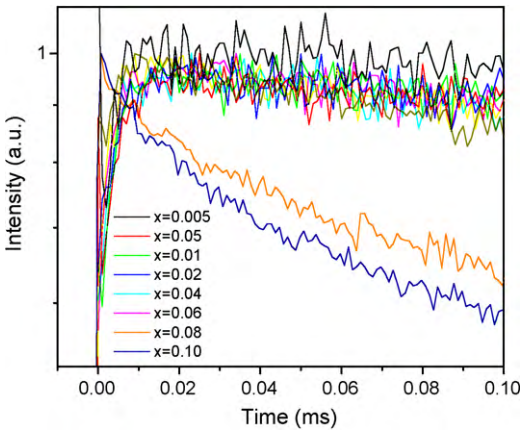

Fig. 5. Enlarged decay curves of $^5D_0$–$^7F_2$ transition of $NaCa_{4-2x}(BO_3)_3$:xEu^{3+},xNa^+.

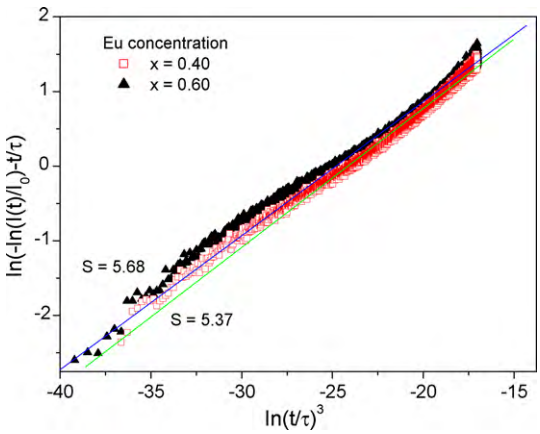

Fig. 6. A plot of the experimental data according to Eq. (2) (Solid lines are theoretical fits and calculated S values are given to each line).

of $^5D_0$ level. For $x < 0.08$, the decay curves are in the form of single exponential decay and the change of decay time with Eu^{3+} concentration can be ignored. The fitted result is about 1.75 ms. Moreover, it should be noted from Fig. 5 that there are two processes in the decay curves for Eu^{3+} emission: build-up process and decay process. Zych et al. reported same results in Lu_2O_3:Eu^{3+} [21]. In general, the appearance of the rise time indicates the presence of a slow relaxation processes feeding the emitting level, and their rise rates should be similarly independent of concentration [21]. However, in this case, the rise time decreases gradually with increasing Eu^{3+} contents, which could be associated with cooperative processes [21]. It is well known that the emission from higher excited $^5D_3$, $^5D_2$, and $^5D_1$ states cannot be observed even at low concentrations of Eu^{3+} ions in high-energy phonon matrixes (e.g., borates and silicates) [22]. In fact, we cannot observe the emissions from $^5D_3$, $^5D_2$, and $^5D_1$ even the Eu^{3+} concentration equals to 0.05 mol%. The mechanism of population of the $^5D_0$ level could be associated with cooperative interactions, predominantly with the cross-relaxation following the scheme [21]

$$^5D_1 \rightarrow {}^5D_0 \leftrightarrow {}^7F_0 \rightarrow {}^7F_2, {}^7F_1 \rightarrow {}^7F_3 \quad (2)$$

The deviation from the single exponential behavior is due to the nonradiative process involving cross-relaxation. Huber [23] shows that the function $f(t)$ describing the decay of donor excitation in the presence of one type of acceptor only and the absence of back transfer, is given by

$$f(t) = \exp\left(\frac{-t}{\tau_R}\right) \times \prod_i (1 - x + x\exp(-(X_{0i} + W_{0i})t) \times \cos\ h(W_{0i}t)) \quad (3)$$

with x the concentration of acceptors, τ_R the radiative decay time. X_{0i} and W_{0i} the trapping rate and the transfer rate between a donor at site 0 and an acceptor at site I, respectively, and Π being the product over all the lattice sites.

In order to verify the nature of the ion interaction in this system, we attempted to analyze the decay curves within the framework of the Inokuti–Hirayama (I–H) model [24]. This approach is formally an approximation of Eq. (3) in assumption of the continuous distribution of the acceptor sites around the donor and the absence of migration amongst the donors. The resulting decay function has the form [24]

$$\frac{I(t)}{I_0} = \exp\left[-\frac{t}{\tau} - \alpha\left(\frac{t}{\tau}\right)^{3/S}\right] \quad (4)$$

where $I(t)$ is the emission intensity after pulsed excitation, I_0 is the intensity of the emission at $t = 0$, τ is the intrinsic lifetime of a single ion, α is a parameter containing the energy probability, and S is an indication of electric multipole character; $S = 6$, 8, 10 for dipole–dipole (DD), dipole–quadrupole (DQ), and quadrupole–quadrupole (QQ) interactions, respectively. For the purpose of getting a correct S value in this case, a plot of [25]

$$\ln\left[-\ln\left(\frac{I(t)}{I_0}\right) - \left(\frac{t}{\tau}\right)\right] \leftrightarrow \ln\left(\frac{t}{\tau}\right)^3 \quad (5)$$

was used. This plot should yield a straight line with a slope equal to $1/S$. Fig. 6 shows fitting results for two different Eu^{3+} concentrations, i.e., $x = 0.40$ and 0.60. The S values are determined to be 5.37 and 5.68. These values are close to the value of 6, so the mechanism of concentration quenching is dipole–dipole interaction. It should also be noted that these values are lower than that of d–d interaction. The deviation from 6 could be attributed to the migration effect between Eu^{3+} ions [25], and this issue is currently under investigation.

4. Conclusions

$NaCa_4(BO_3)_3$ doped with Eu^{3+} phosphors have been synthesized by solid-state reactions. The emission spectra exhibit the well-known transitions from $^5D_0$ level to $^5D_0 \rightarrow {}^7F_0$, $^5D_0 \rightarrow {}^7F_1$, $^5D_0 \rightarrow {}^7F_2$, $^5D_0 \rightarrow {}^7F_3$, and $^5D_0 \rightarrow {}^7F_4$. The excitation spectrum consists of broad charge transfer transition of Eu^{3+}–O^{2-} and Eu^{3+} intra-$4f^6$ transitions, i.e., 320 nm ($^7F_0$–^5H_J), 396 nm ($^7F_0$–$^5L_6$), and 465 nm ($^7F_0$–$^5D_2$). The optimum Eu^{3+} concentration is 8 mol%, and the calculated critical distance of the concentration quenching is 16.7 Å. The fitted fluorescence lifetime is 1.75 ms, and the mechanism of concentration quenching derived from decay curves is dipole–dipole interaction.

Acknowledgements

This work was supported by Youth Scientific Research Foundation of Central South University of Forestry and Technology (No. 2009009A). This work was also financially supported by the Korea Science and Engineering Foundation (KOSEF) grant funded by the Korea government (MEST) (No. 2009-0078682).

References

[1] X. Chen, C. Yang, X. Chang, H. Zang, W. Xiao, J. Alloys Compd. 492 (2010) 543.
[2] P. Li, L. Pang, Z. Wang, Z. Yang, Q. Guo, X. Li, J. Alloys Compd. 478 (2009) 813.
[3] L.H. Jiang, Y.L. Zhang, C.Y. Li, J.Q. Hao, Q. Su, J. Alloys Compd. 482 (2009) 313.
[4] Y. Huang, W. Zhao, L. Shi, H.J. Seo, J. Alloys Compd. 477 (2009) 936.
[5] E.-J. Popovici, M. Nazarov, L. Muresan, D.Y. Noh, L.B. Tudoran, E. Bica, E. Indrea, J. Alloys Compd. 497 (2010) 201.
[6] A. Majchrowski, S. Klosowicz, L.R. Jaroszewicz, M. Swirkowicz, I.V. Kityk, M. Piasecki, M.G. Brik, J. Alloys Compd. 491 (2010) 26.

[7] M.A.K. Elfayoumi, M. Farouk, M.G. Brik, M.M. Elokr, J. Alloys Compd. 492 (2010) 712.
[8] A.S. Aleksandrovsky, I.A. Gudim, A.S. Krylov, A.V. Malakhovskii, V.L. Temerov, J. Alloys Compd. 496 (2010) L18.
[9] M.M. Haque, H.-I. Lee, D.-K. Kim, J. Alloys Compd. 481 (2009) 792.
[10] X.M. Zhang, H. Chen, W.J. Ding, H. Wu, J.S. Kim, J. Am. Ceram. Soc. 92 (2009) 429.
[11] L. Wu, X.L. Chen, Y.P. Xu, Y.P. Sun, Inorg. Chem. 45 (2006) 3042.
[12] L. Jiang, Y. Zhang, C. Li, R. Pang, L. Shi, S. Zhang, J. Hao, Q. Su, J. Rare Earths 27 (2009) 320.
[13] J.L. Huang, L.Y. Zhou, Z.L. Wang, Y.W. Lan, Z.F. Tong, F.Z. Gong, J.H. Sun, L.P. Li, J. Alloys Compd. 487 (2009) L5.
[14] Y. Huang, L. Shi, E.S. Kim, H.J. Seo, J. Appl. Phys. 105 (2009) 013512.
[15] Y. Huang, W. Zhao, Y. Cao, K. Jang, H.S. Lee, E. Cho, S.S. Yi, J. Solid State Chem. 181 (2008) 2161.
[16] Y. Huang, C. Jiang, Y. Cao, L. Shi, H.J. Seo, Mater. Res. Bull. 44 (2009) 793.
[17] J.H. Zhang, H.B. Liang, Q. Su, J. Phys. D 42 (2009) 105110.
[18] P. Dorenbos, J. Lumin. 111 (2005) 89.
[19] B. Saubat, C. Fouassier, P. Hagenmuller, J.C. Bourcet, Mater. Res. Bull. 16 (1981) 193.
[20] G. Blasse, Philips Res. Rep. 24 (1969) 131.
[21] E. Zych, D. Hreniak, W. Strek, J. Phys. Chem. B 106 (2002) 3805.
[22] G. Blasse, B.C. Grabmaier, Lumin. Mater., Springer, Berlin, 1994.
[23] D.L. Huber, Phys. Rev. B 20 (1979) 2307.
[24] M. Inokuti, F. Hirayama, J. Chem. Phys. 43 (1965) 1978.
[25] K.S. Sohn, Y.Y. Choi, H.D. Park, J. Electrochem. Soc. 147 (2000) 1988.